

# Load Carrying Capacity of Screw Helical Gears with Steel Pinions and Plastic Wheels

Wolfgang Predki and Peter Barton

## Management Summary

There is an increasing significance of screw helical and worm gears that combine use of steel and plastics. This is shown by diverse and continuously rising use in the automotive and household appliance industries. The increasing requirements for such gears can be explained by the advantageous qualities of such a material combination in comparison with that of the traditional steel/bronze pairing.

In order to develop an optimal design of steel/plastic gears in the future, a comprehensive and systematic calculation method has been developed. It enables the designer to calculate the operating life and the load capacity for diverse operating and design parameters. The calculation method is based on several experimental and theoretical considerations, by which the influence of various parameters on efficiency and damage mechanisms is tested.

## Abstract

The development of a new calculation process has for the first time made it possible to calculate the load carrying capacity of screw helical gears with steel pinions and plastic wheels. This development has laid the foundation for a technically and economically optimized design of future gear unit generations. The calculation process is based on numerous theoretical and experimental investigations.

## Introduction

Screw helical gears in which the wheel is made from plastic and the pinion which engages a cylindrical worm is made from steel are being used increasingly in drive engineering. For example, gear units of this type are used in the automotive industry, in drives for electric window lifters and windscreen wipers, in electric seat adjustment systems, and are used in domestic appliances, such as the electrical bread slicer.

These applications are making use of the advantages offered by this material combination in comparison to a conventional steel/bronze pairing. The advantages include reduced weight, lower manufacturing costs and good vibration damping characteristics. Other advantages are the reduced lubrication requirements and the high level of electrical insulation.

These advantages could not be exploited to the optimum extent in the past because the load carrying capacity of screw helical gears with steel pinions and plastic wheels could only be estimated, not calculated accurately (Refs. 5–6).

The objective of this research project, only the salient points of which are presented here, was therefore to conduct theoretical and experimental investigations as a means for analyzing the load carrying capacity of these gear units. This would allow for development of a calculation method and a computer program, which for the first time would enable designers to accurately calculate and, in the final analysis, optimize the load carry-

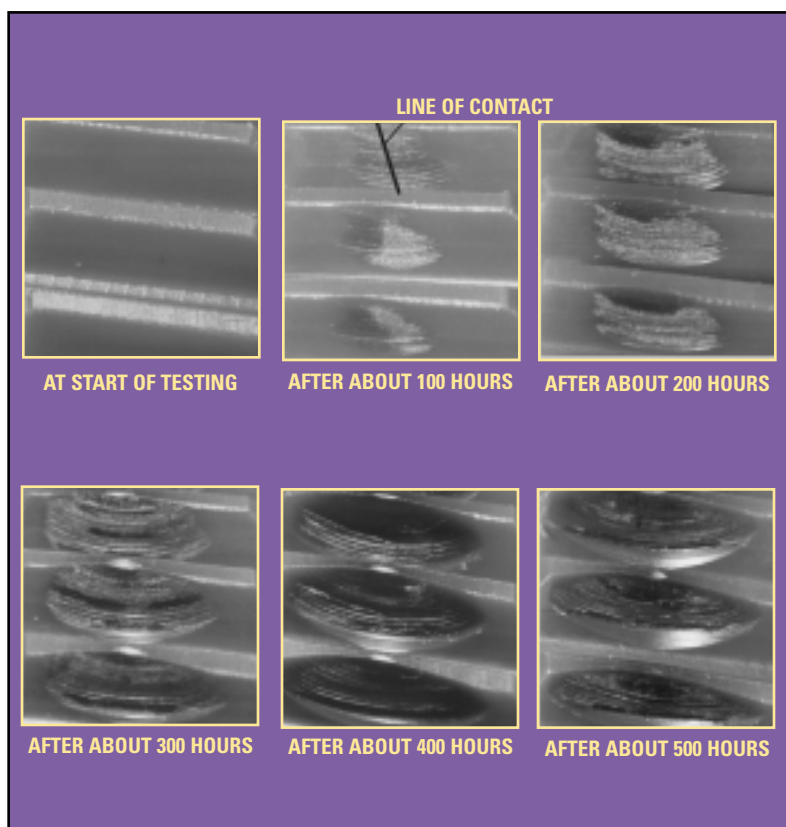


Figure 1—Wear.

ing capacity and operating life of the gear units.

This paper not only presents a means for calculating tooth coefficients of friction, it also presents a means for estimating permitted tooth temperatures and allowable extent of wear. A detailed presentation of this topic can be found in Reference 1. This reference deals in greater depth with load carrying capacity at the tooth root and with pitting, as well as the temperature fluctuations in the lubricant.

### Gear Damage

Various types of gear damage occurred during the numerous experiments conducted to calculate the load carrying capacity of the aforementioned screw helical gears. These damages led to the total failure of the gear units.

The series of photographs in Figure 1 show tooth flanks at various stages of an endurance test, starting at the beginning of the test and after approximately 100, 200, 300, 400 and 500 hours of running. As well as the position of the line of contact, the propagation of the contact pattern can be seen clearly. This indicates the increasing degree of wear.

Figure 2 shows how the plastic teeth break along the addendum circle of the worm. As a result of the notch effect, the crack either starts in the middle of the tooth or on the addendum circle of the worm at the level of the gear's datum circle.

The deformation of the gear teeth results in a pinching effect within the gearing, as shown in Figure 3.

Excessive temperatures lead to melting of the gearing, as shown in Figure 4.

Also, pitting, as seen in Figure 5, leads to vibration of the gear unit, causing additional undesirable dynamic forces.

### Analysis of Load Carrying Capacity

An extensive analysis of the load carrying capacity is needed in order to preclude the aforementioned damage mechanisms. As a result, the individual damage modes are incorporated into the newly developed equations.

**Ascertaining the average tooth coefficient of friction  $\mu_{zm}$ .** The analysis of the load carrying capacity starts by ascertaining the average tooth coefficient of friction  $\mu_{zm}$ . This determines the losses in the gearing and is used for ascertaining the gearing power loss  $P_{vz}$ .

In Figure 6, the diagram shows sample  $\mu_{zm}$  values for various speeds and torques. These are calculated on the basis of torque and speed measurements during the tests, with consideration for losses in bearings and on seals on the basis of the

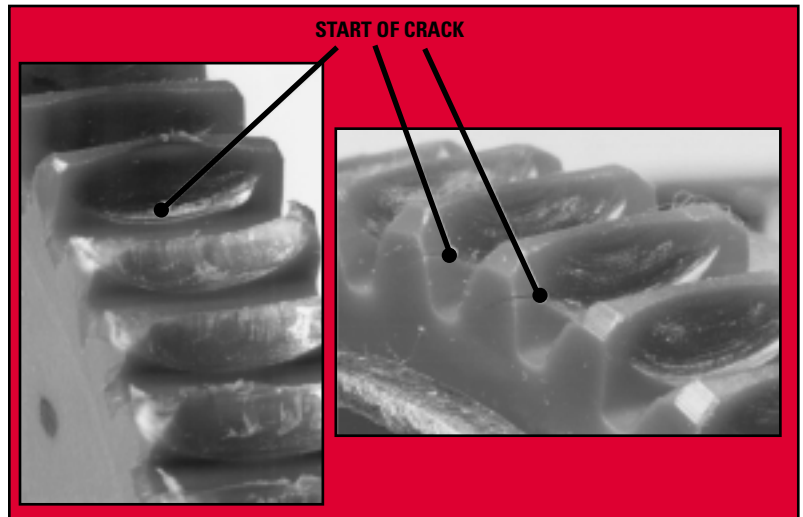


Figure 2—Tooth break.

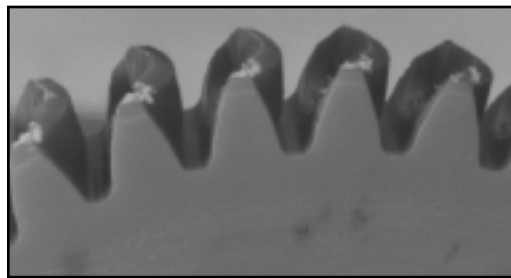


Figure 3—Deformation of the gear teeth.

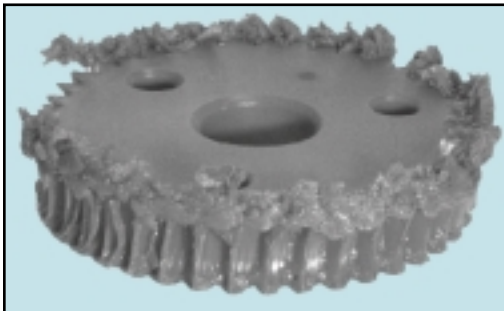


Figure 4—Melting.

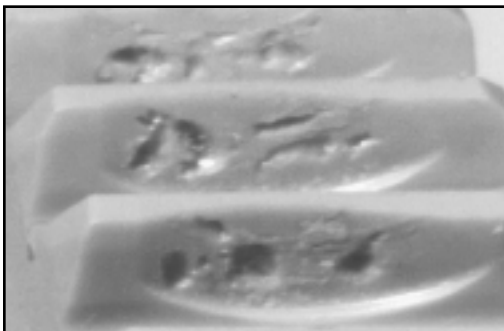


Figure 5—Pitting

manufacturer's figures.

As can be seen, the values for the average tooth coefficient of friction increase as the speed increases and the torque is reduced.

The curves shown are the results of regression calculations. The equations described for the average tooth coefficient of friction  $\mu_{zm}$  are listed

### Prof. Dr.-Ing. Wolfgang Predki

is the head of the chair of mechanical components, industrial and automotive power transmission at Ruhr University, located in Bochum, Germany. The chair's research focuses on wear optimization of worm gears, on plastic and sintered worm gears and on optimization of bronze gears.

### Dr.-Ing. Peter Barton

is a department head at SEW-Eurodrive GmbH & Co. KG in Bruchsal, Germany. His department performs research & development for industrial gears, specifically helical, bevel-helical and planetary gearboxes, as well as customized designs. At SEW, he's performing basic research in Spiroplan® gearboxes, which are similar to the screw helical gears discussed in this paper. The paper itself summarizes parts of his Ph.D. dissertation.

as Equations 1 and 2 (Ref. 1). The datum circle is used for calculating the average tooth coefficient of friction in screw helical gears in a similar manner to the process for worm gear units (Ref. 2). The sliding speed at the datum circle is then calculated according to DIN 3996 (Ref. 3).

$$\mu_{zm,PEEK} = 0.0549 + 0.0334 \cdot v_{gm}^{0.4817} + 0.2528 \cdot T_2^{-2.2462} - 0.027 \cdot \left( \frac{v_{gm} \cdot T_2}{a} \right)^{1.1323} \quad (1)$$

$$\mu_{zm,PA4.6} = 0.0907 + 0.0314 \cdot v_{gm}^{0.4485} + 0.1904 \cdot T_2^{-2.1227} - 0.0598 \cdot \left( \frac{v_{gm} \cdot T_2}{a} \right)^{0.3902} \quad (2)$$

$\mu_{zm,PEEK}$  : Average tooth coefficient of friction for the PEEK material

$\mu_{zm,PA4.6}$  : Average tooth coefficient of friction for the PA4.6 material

$v_{gm}$  : Sliding speed at the datum circle in m/s

$T_2$  : Output torque in Nm

$a$  : Center distance in mm

**Temperature equations.** A preliminary thermal calculation for screw helical gears with steel pinions and plastic wheels forms the basis for a more accurate investigation of the individual damage mechanisms.

It is possible to assess the functional capabilities of the lubrication system by determining the sump temperature; the gear mass temperature provides information about the strength of the gear material in the tooth core, while the flank temperature makes it possible to analyze the material strength at the surface of the flank.

Since the procedures for ascertaining the individual temperatures are practically identical, only the process for ascertaining the flank temperature  $\vartheta_{VZ}$  is shown here by way of example.

The flank temperature  $\vartheta_{VZ}$  is the maximum temperature which arises in the gear unit, because it is measured directly at the principal point of heat generation, namely on the tooth flank. It is composed of the sump temperature  $\vartheta_s$  and the excess flank temperature  $\Delta\vartheta_{VZ}$ . The approximation equations for the excess flank temperature are listed in Equations 3 and 4; these are dependent on the material.

$$\Delta\vartheta_{VZ,PEEK} = 0.3866 \cdot P_{VZ} + 43,755.264 \left( \frac{T_2}{a^2 \cdot u} \right) v_{gm}^{1.1938} \quad (3)$$

$$\Delta\vartheta_{VZ,PA4.6} = 0.0579 \cdot P_{VZ} + 69,582.462 \left( \frac{T_2}{a^2 \cdot u} \right) v_{gm}^{1.2353} \quad (4)$$

$\Delta\vartheta_{VZ,PEEK}$  : Excess flank temperature for the PEEK material in °C

$\Delta\vartheta_{VZ,PA4.6}$  : Excess flank temperature for the PA4.6 material in °C

$P_{VZ}$  : Gearing power loss in W

$T_2$  : Output torque in Nm

$a$  : Center distance in mm

$u$  : Ratio =  $z_2/z_1$

$v_{gm}$  : Sliding speed at the datum circle in m/s

The gearing power loss  $P_{VZ}$  is calculated according to DIN 3996 (Ref. 3) with incorporation of Equations 1 and 2.

Figure 7 indicates that the excess flank temperature increases as the speed and torque

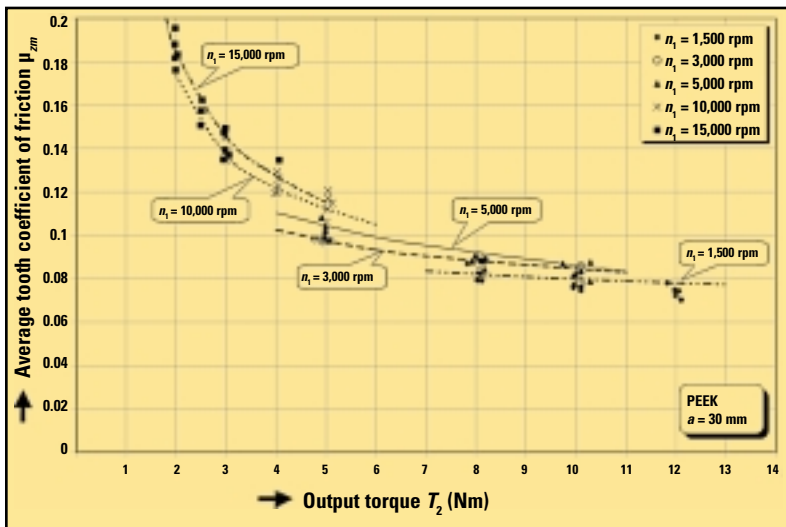


Figure 6—Average tooth coefficient of friction  $\mu_{zm}$ .

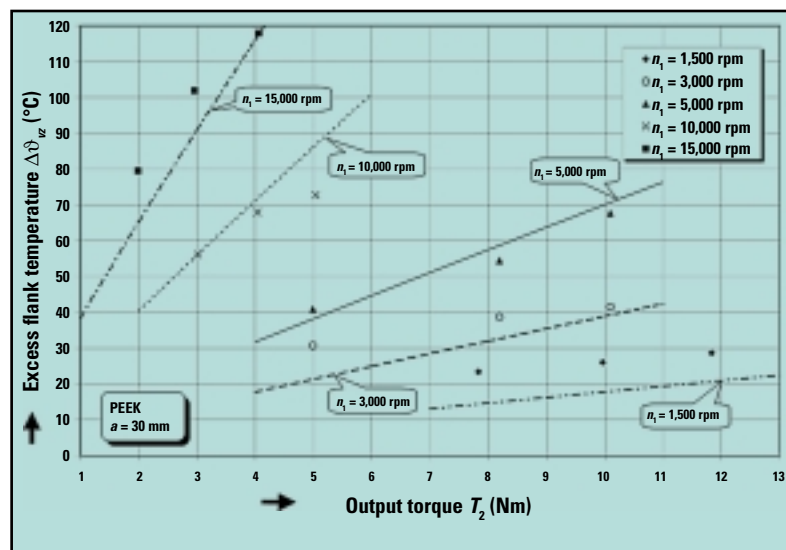


Figure 7—Excess flank temperature.

increase. The approximation equations for the particular materials are listed in Equations 3 and 4.

**Extent of wear.** Wear represents a significant mode of damage. The calculation of wear is illustrated here by way of example. The extent of wear in the normal plane  $\delta_{wn}$  is introduced for the purposes of the calculation process. In the calculation model, the actual progression of the wear is replaced by a fixed running-in wear  $\delta_{w0n}$  and an increase in wear  $\delta_{dwn}$ , which depends on the operating time.

The extent of wear increases over time, as shown in Figure 8. Starting from zero, the wear increases rapidly during the first few hours before starting a less pronounced, almost linear progression.

The resulting calculation method is shown in Equation 5.

$$\delta_{wn} = \delta_{w0n} + \delta_{dwn} \quad (5)$$

- $\delta_{wn}$  : Extent of wear in normal plane in  $\mu\text{m}$
- $\delta_{w0n}$  : Running-in wear in normal plane in  $\mu\text{m}$
- $\delta_{dwn}$  : Increase in wear in normal plane in  $\mu\text{m}$

The following equations are used for determining the amount of wear. It is first necessary to ascertain the running-in wear, followed by the increase in wear.

**Running-in wear.** The running-in wear is calculated using Equations 6 and 7; it is represented as a function of the Hertzian compressive load for screw helical gears at ambient temperature. At an elevated ambient temperature, the compressive load must be ascertained using the starting temperature.

Investigations have shown that it is a good idea to use the surface stress at ambient temperature because there is no temperature equilibrium and therefore no stress equilibrium established during the period in which running-in wear takes place.

The effect of the ratio is taken into account in the equations by the coefficient of the average sliding distance  $s^*$ . The Hertzian surface stress at ambient temperature  $\sigma_{Hm0S}$  has to be ascertained on the basis of the Niemann/Winter Theory (Ref. 4), while the coefficient of the average sliding distance  $s^*$  is ascertained according to DIN 3996 (Ref. 3).

$$\delta_{w0n,PEEK} = (2.2458 \cdot v_{gm}^{0.5206} + (0.015 \cdot \sigma_{Hm0S})^{3.8835}) \cdot \left( \frac{s^*}{44.7678} \right)^{2.3716} \quad (6)$$

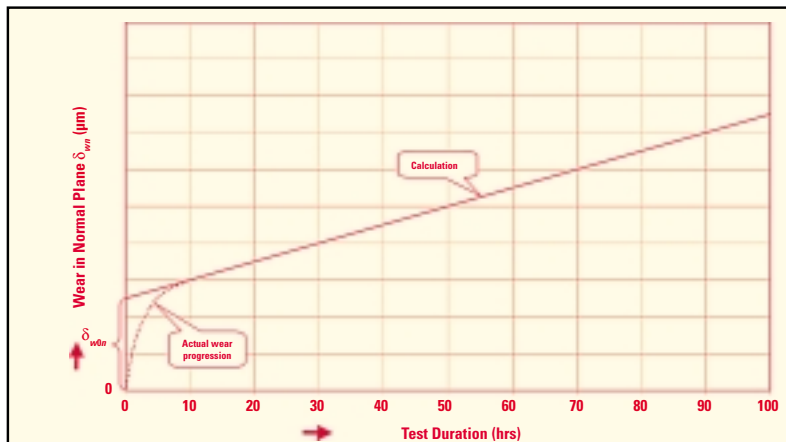


Figure 8—Extent of wear.

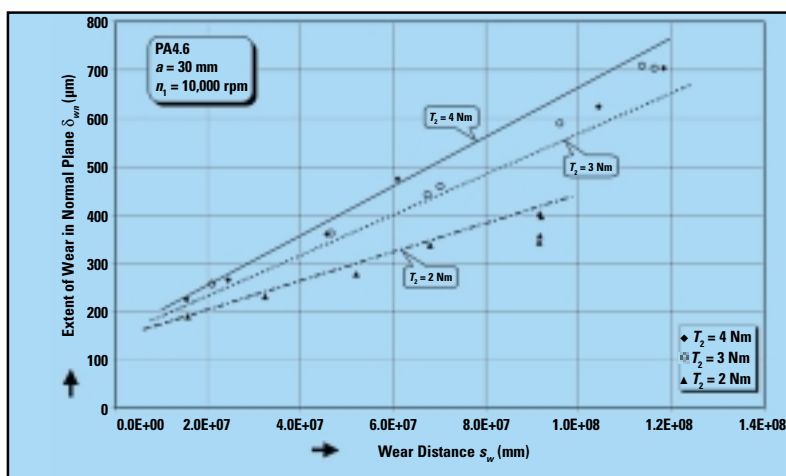


Figure 9—Wear measuring results.

$$\delta_{w0n,PA4.6} = (7.3625 \cdot v_{gm}^{1.5724} + (0.0205 \cdot \sigma_{Hm0S})^{2.9419}) \cdot \left( \frac{s^*}{45.0917} \right)^{2.3968} \quad (7)$$

- $\delta_{w0n,PEEK}$  : Running-in wear in normal plane for the PEEK material in  $\mu\text{m}$
- $\delta_{w0n,PA4.6}$  : Running-in wear in normal plane for the PA4.6 material in  $\mu\text{m}$
- $v_{gm}$  : Average sliding speed at the datum circle in m/s
- $\sigma_{Hm0S}$  : Hertzian surface stress at ambient temperature in  $\text{N}/\text{mm}^2$
- $s^*$  : Coefficient of the average sliding distance

**Increase in wear.** DIN 3996 (Ref. 3) provides a calculation method for the increase in wear  $\delta_{dwn}$ . This can be calculated in accordance with Equation 8 by taking the wear intensity  $J_w$  and the wear distance  $s_w$ . The wear distance  $s_w$  can be calculated according to DIN 3996 (Ref. 3).

$$\delta_{dwn} = J_w \cdot s_w \quad (8)$$

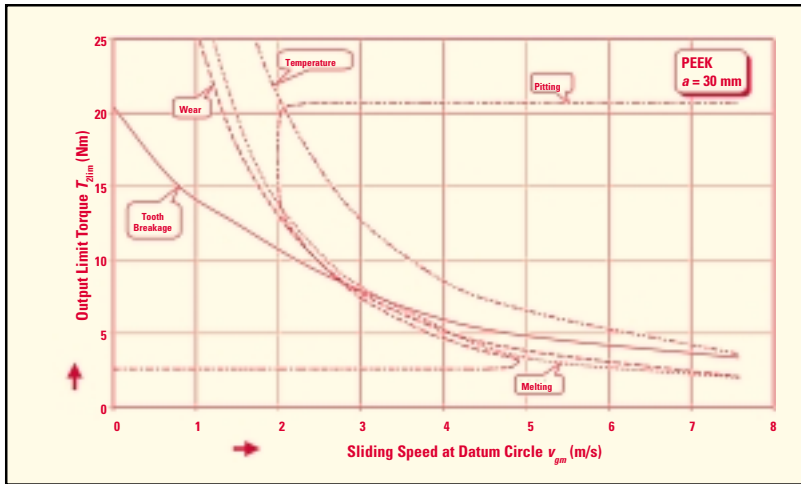


Figure 10—Output limiting torque curves.

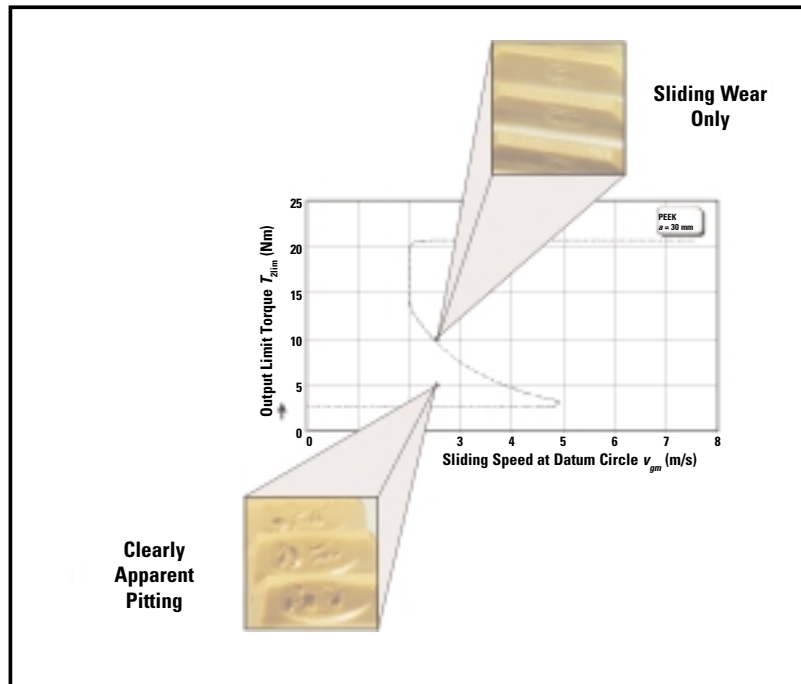


Figure 11—Pitting limit torque curve.

$\delta_{dwn}$  : Increase in wear in normal plane in  $\mu\text{m}$

$J_w$  : Wear intensity

$s_w$  : Wear distance in mm

The wear intensity  $J_w$  depends on the Hertzian surface stress in worm gear units  $\sigma_{HmG}$  according to DIN 3996 (Ref. 3), the average sliding speed  $v_{gm}$ , the center distance  $a$  and the lubricant viscosity  $\nu$  at operating temperature, see Equations 9 and 10.

$$J_{w,PEEK} = 4.9228 \cdot 10^{-5} \cdot \sigma_{HmG}^{0.1717} \cdot v_{gm}^{-0.1952} \cdot a^{-0.5513} \cdot \nu^{-0.4713} \quad (9)$$

$$J_{w,PA4.6} = 1.7165 \cdot 10^{-5} \cdot \sigma_{HmG}^{1.0843} \cdot v_{gm}^{0.3248} \cdot a^{-1.101} \cdot \nu^{-0.3866} \quad (10)$$

$J_{w,PEEK}$  : Wear intensity for the PEEK material

$J_{w,PA4.6}$  : Wear intensity for the PA4.6 material

$\sigma_{HmG}$  : Average surface stress on worm gears in  $\text{N/mm}^2$

$v_{gm}$  : Sliding speed at the datum circle in m/s

$a$  : Center distance in mm

$\nu$  : Kinematic viscosity of the lubricant at operating temperature in  $\text{mm}^2/\text{s}$

The wear intensity increases as the compressive load increases and as the center distance and the lubricant viscosity decrease.

The wear measuring results and the approximations in Equations 5, 7, 8 and 10 are shown by way of example in Figure 9 for a screw helical gear with PA4.6 as the wheel material, a center distance of  $a = 30$  mm and an input speed of  $n_1 = 10,000$  rpm.

Two wear limits can be specified for ascertaining the safety margin: 1.) when a gear tooth becomes pointed, because further wear would lead to a reduction in the tooth height and 2.) excessive backlash, which is specified as  $0.3 \cdot m_n$ , according to DIN 3996 (Ref. 3).

#### Simulation with the KSG Computer Program

For the first time, the newly developed KSG computer program makes it possible for designers to simulate screw helical gears with steel pinions and plastic wheels, i.e. to calculate the load carrying capacity and operating life. Figure 10 shows examples of size  $a = 30$  mm gear units with the PEEK material, the limit curves for the output torque as a function of the sliding speed at the datum circle  $v_{gm}$  and the damage mechanisms.

In the lower speed range, the tooth breakage damage mechanism is the limiting factor, while wear comes to prominence in the medium range. At high speed, melting is the decisive factor influencing the level of torque which can be transmitted. The temperature of the lubricant does not have a limiting effect provided the lubricant is suitable. Pitting occurs in the lower and medium speed ranges even at low levels of wear; however, this does not lead directly to failure of the gearing. As a result, pitting is not regarded as a limiting factor.

The pitting limit curve in Figure 10 differs from the other curves in terms of its shape. This is because of the non-definitive area in the medium speed range. In other words, in a gear that undergoes pitting at low torque levels, pitting can be avoided by increasing the output torque. The

reason for this lies in the considerable drop in the  $e$ -modulus of the plastic at the glass transition temperature, an effect which comes fully into play in this example.

Figure 11 illustrates this phenomenon. In this case, the pitting limit curve and the tooth flanks from two experiments are shown at the same operating time. The lower section shows a gear which was subjected to an output torque of 5 Nm and displays clearly apparent pitting. However, doubling the output torque to 10 Nm results in only sliding wear.

### Conclusion

For the first time, the calculation method presented briefly here permits designers to accurately calculate the load carrying capacity of screw helical gears with steel pinions and plastic wheels. As a result, the process allows these drives to be optimized. Test rig trials conducted on size  $a = 30$  mm and  $a = 65$  mm gear units served to investigate the influence of various design and operating parameters on the load carrying capacity of the gear unit.

The test gear units were fitted with cylindrical worms with ground tooth flanks and wheels made from PEEK and PA4.6. The speed and torque were varied in addition to the geometries and the materials.

On the basis of the gear unit losses, it is possible as a first step to determine approximation equations for the average tooth coefficient of friction. These equations serve as the basis for temperature calculations. At the same time, static evaluation of the measured temperatures results in approximation equations for the sump, gear mass and flank temperatures. This shows that the temperatures are dependent on the gearing power losses, the output torque in relation to the center distance and the gear tooth ratio, as well as the sliding speed at the datum circle.

It is possible to determine the extent of wear on the tooth flanks on the basis of the temperature equations which were obtained. To a large degree, the extent of wear influences the load carrying capacity of the gearing.

The load carrying capacity of the tested gear units is significantly dependent on the worm speed, the torque and the material. These test parameters give rise to different gear damage. There are increased levels of pitting and tooth breakage at low speed. At high speeds, the gear unit fails due to the upper operating temperature of the plastic or the lubricant being exceeded. As a rule, gears made from PA4.6 do not have as

great a load carrying capacity as those made from PEEK.

Finally, the newly developed KSG simulation program enables the user to preclude the various aforementioned types of damage and to optimally design the gear unit in view of the required boundary conditions. ⚙

**This paper was presented at the VDI symposium "Maschinenelemente aus Kunststoff," held Oct. 10, 2001, in Erlangen-Nürnberg, Germany, and at the International Conference on Gears, held March 13–15, 2002, in Munich, Germany. It was also published by VDI Verlag GmbH in the conference's proceedings, in VDI report 1665. It is republished here with VDI Verlag's permission.**

### References

1. Barton, P. "Tragfähigkeit von Schraubrad- und Schneckengetrieben der Werkstoffpaarung Stahl/Kunststoff," Ph.D. Dissertation, Ruhr-Universität Bochum, Deutschland, 2000.
2. DIN 3975. "Begriffe und Bestimmungsgrößen für Zylinderschneckengetriebe mit Achsenwinkel  $90^\circ$ ," Beuth Verlag GmbH, Berlin, Deutschland, July 2002.
3. DIN 3996. "Tragfähigkeit von Zylinder-Schneckengetrieben mit Achsenwinkel =  $90^\circ$ ," Beuth Verlag GmbH, Berlin, Deutschland, September 1998.
4. Niemann, G., and H. Winter. *Maschinenelemente Band III*, 2nd ed., Springer Verlag, Berlin, Deutschland, 1986.
5. Schmidt, H. "Schneckengetriebe mit Schneckenrädern aus Hostaform," *Antriebstechnik*, Vol. 24, No. 3, March 1985, pp. 61–67.
6. VDI Richtlinie 2545. "Zahnräder aus thermoplastischen Kunststoffen," VDI-Verlag GmbH, Düsseldorf, Deutschland, January 1981.

**Tell Us What You Think . . .**

**E-mail [wrs@geartechnology.com](mailto:wrs@geartechnology.com) to**

- **Rate this article**
- **Request more information**
- **Contact the authors or organizations mentioned**
- **Make a suggestion**

**Or call (847) 437-6604 to talk to one of our editors!**